

An analytical approach to probabilistic modeling of liquefaction based on shear wave velocity

A. Johari¹, A.R. Khodaparast¹, A.A. Javadi²

1- Department of Civil and Environmental Engineering, Shiraz University of Technology, Shiraz, Iran

2- Computational Geomechanics Group, Department of Engineering, University of Exeter, Exeter, EX4 4QF, UK
johari@sutech.ac.ir

Abstract

Evaluation of liquefaction potential of soils is an important step in many geotechnical investigations in regions susceptible to earthquake. For this purpose, the use of site shear wave velocity (V_s) provides a promising approach. The safety factors in the deterministic analysis of liquefaction potential are often difficult to interpret because of uncertainties in the soil and earthquake parameters. To deal with the uncertainties, probabilistic approaches have been employed. In this research, the Jointly Distributed Random Variables (JDRV) method is used as an analytical method for probabilistic assessment of liquefaction potential based on measurement of site shear wave velocity. The selected stochastic parameters are stress-corrected shear-wave velocity and stress reduction factor, which are modeled using a truncated normal probability density function and the peak horizontal earthquake acceleration ratio and earthquake magnitude, which are considered to have a truncated exponential probability density function. Comparison of the results with those of Monte Carlo Simulation (MCS) indicates very good performance of the proposed method in assessment of reliability. Comparison of the results of the proposed model and a Standard Penetration Test (SPT)-based model developed using JDRV shows that shear wave velocity (V_s)-based model provides a more conservative prediction of liquefaction potential than the SPT-base model.

Keywords: Reliability, Jointly distributed random variables method, Monte Carlo simulation, Liquefaction, Shear wave velocity

1. Introduction

Liquefaction results from tendency of soil deposits to decrease in volume when subjected to shearing stresses. In a deterministic analysis, liquefaction can be determined using the Cyclic Resistance Ratio (CRR) and Cyclic Stress Ratio (CSR) due to earthquake (Kramer 1996). The cyclic stress ratio is obtained using some soil and earthquake characteristics (Seed and Idriss 1971). The cyclic resistance ratio can be obtained by several methods that were proposed by Seed and Idriss (1971), or as demonstrated by Youd and Idriss (2001), using the standard penetration test (Seed, Tokimatsu et al. 1984, Bolton Seed, Tokimatsu et al. 1985, Arulanandan, Yogachandran et al. 1986, Seed and De Alba 1986, Seed and Harder 1990, Youd, Idriss et al. 2001), cone penetration test (Arulanandan, Yogachandran et al. 1986, Seed and De Alba 1986, Mitchell and Tseng 1990, Robertson 1990, Juang and Chen 1999, Youd, Idriss et al. 2001, Baziar and Nilipour 2003, Juang, Yuan et al. 2003, Lees et al. 2015), triaxial test results (Silver 1977), or shear wave velocity (Andrus and Stokoe 1997, Andrus and Stokoe II 2000).

Evaluation of soil liquefaction using site shear wave velocity provides a more applicable method than other site test methods such as standard penetration and cone penetration tests. This method is particularly useful for specific soils such as gravel where penetration tests may be unreliable, and at sites where borings may not be permitted such as under constructed structure and landfill (Dobry, Stokoe et al. 1981, Seed, Idriss et al. 1983, Stokoe, Roesset et al. 1988, Tokimatsu and Uchida 1990). However, Andrus et al. (2004) pointed out that this method is more conservative than penetration-based methods for evaluation of liquefaction for the compiled Holocene data. Youd and Idriss (2001) and Andrus et al. (2004) provide further discussion on the advantages and disadvantages of this method and penetration-based methods in evaluation of liquefaction potential.

However, the inherent uncertainties of the parameters, which affect liquefaction, dictate that this problem is of a probabilistic nature rather than being deterministic. Uncertainty in liquefaction can be divided into two distinctive categories: uncertainty in the cyclic stress ratio

1 due to earthquake characteristics and uncertainty in the cyclic resistance ratio due to soil
2 properties. In the first category, the selection of appropriate earthquake parameters such as
3 magnitude, location and recurrence to assess the liquefaction potential of the site would be
4 important and in second category, the parameter uncertainty, model uncertainty and human
5 uncertainty would be important (Morgenstern 1995). Parameter uncertainty is the uncertainty
6 in the input parameters for analysis (Ishihara 1996); model uncertainty is due to the limitation
7 of the theories and models used in performance prediction (Whitman 2000), while human
8 uncertainty is due to human errors and mistakes (Sowers 1991).

9 Reliability analysis provides a means of evaluating the combined effects of uncertainties
10 and offers a logical framework for choosing factors of safety that are appropriate for the degree
11 of uncertainty and the consequences of failure. Thus, as an alternative or a supplement to the
12 deterministic assessment, a reliability assessment of liquefaction potential would be useful in
13 providing better engineering decisions.

14 There are many reliability approaches that have been developed to deal uncertainties in
15 liquefaction potential based on shear wave velocity. These approaches can be grouped into three
16 categories: approximate methods, artificial intelligence method and regression analysis.

17 **Approximate methods:** Most of the approximate methods are modified versions of three
18 methods namely, First Order Second Moment (FOSM) method (Alfredo and Wilson 1975), Point
19 Estimate Method (PEM) (Rosenblueth 1975), and First Order Reliability Method (FORM)
20 (Hasofer, Lind et al. 1973). These approaches require knowledge of the mean and variance of all
21 input variables as well as the performance function that defines liquefaction safety factor.

22 Juang et al. (2005) used FORM to characterize the uncertainty of a shear wave velocity-based
23 simplified model for liquefaction potential evaluation developed by Andrus and Stokoe (1997,
24 2000). They represented the uncertainty of this simplified model by a lognormal random variable
25 and performed a trial-and-error procedure to determine the two statistical parameters of the
26 model uncertainty (mean and the Coefficient of Variation (COV)) based on a Bayesian mapping
27 function that was calibrated with a database of case histories.

28 Zou et al. (2017) used FORM to characterize the uncertainty of a Cone penetration test model
29 for liquefaction potential evaluation. It was shown that the deterministic nature of the CPTU
30 observations can be captured in the probabilistic analysis if the proposed procedure is applied.

31 **Artificial intelligence method:** In recent years, by pervasive developments in computational
32 software and hardware, several alternative computer-aided pattern recognition approaches have
33 emerged. The main idea behind pattern recognition systems such as neural network, fuzzy logic
34 or genetic programming is that they learn adaptively from experience and extract various
35 discriminates, each appropriate for its purpose. Artificial Neural Networks (ANNs) and Multi-
36 Layer Regression (MLR) are the most widely used pattern recognition procedures that have been
37 introduced for determination of liquefaction potential. In this approach the reliability analysis is
38 done based on a function that is developed by an appropriate artificial intelligence method (Chau
39 and Wu 2010, Wu, Chau et al. 2010, Taormina, Chau et al. 2015).

40 Juang et al. (2001) developed a new V_s -based empirical equation for assessing the liquefaction
41 resistance of soils using a neural network. A database of case histories was used to train and test
42 an artificial neural network model. The model could predict the occurrence/nonoccurrence of
43 liquefaction based on soil and seismic load parameters. Based on this deterministic model,
44 probabilistic analysis of the cases in the database was conducted using the logistic regression
45 approach and the mapping function approach.

46 Goh (2002) used a Probabilistic Neural Network (PNN) approach based on the Bayesian
47 classifier method to evaluate seismic liquefaction potential based on actual field records and
48 performed two separate analyses, one based on cone penetration test data and one based on
49 shear wave velocity data. Comparisons of the results showed that the PNN models perform far
50 better than the conventional methods in predicting the occurrence or non-occurrence of
51 liquefaction.

1 Muduli et al. (2014) evaluated liquefaction potential of soil within a probabilistic framework
2 based on the post-liquefaction Cone Penetration Test (CPT) data using an evolutionary artificial
3 intelligence technique, multi-gene genetic programming (MGGP).

4 **Regression analysis:** The rationality of the reliability analysis results largely depends on the
5 amount and quality of the collected data used to deduce the statistics of the cyclic soil strength.
6 This method requires collecting data for liquefaction and non-liquefaction cases.

7 Juang et al. (2002) used two different approaches, logistic regression and Bayesian mapping
8 functions for calculating probabilities of liquefaction based on the standard penetration test, cone
9 penetration test, and shear wave velocity measurements and compared the results with each
10 other. They showed that the Bayesian mapping approach is preferred over the logistic regression
11 approach for estimating the site-specific probability of liquefaction, although both methods yield
12 comparable probabilities.

13 Nafday (2010) developed a soil liquefaction models based on survival analysis parametric
14 regression to evaluate the factor of safety and probability of liquefaction.

15 In addition to the above mentioned approaches, analytical methods such as jointly distributed
16 random variables method and numerical methods like Monte Carlo simulation (Metropolis and
17 Ulam 1949, Metropolis and Ulam 1949) also can be employed for reliability analysis of
18 liquefaction potential based on in situ shear wave velocity measurement.

19 In this research, the jointly distributed random variables method is used as an analytical
20 method to assess the reliability of the safety factor in the prediction of liquefaction potential
21 considering the uncertainties in parameters and Monte Carlo simulation is used for verifying the
22 results of JDRV method.

23 In this analytical method, the derivation is done only once and after that, it can be used in
24 many applications. It is also worth noting that, in some problems such as liquefaction potential
25 assessment, when a relatively large number of variables are involved, the Monte Carlo simulation
26 may require hundreds of thousands of simulation runs that make the method excessively
27 demanding in computational time and resources. Moreover, the jointly distributed random
28 variables method can be used for stochastic parameters with any distribution curve (such as
29 normal, exponential, gamma, uniform, ...) whereas some other analytical methods like PEM, and
30 FOSM require specific (e.g., normal) distribution functions. This ability is very important because
31 the peak horizontal earthquake acceleration ratio (α) and earthquake magnitude (M_w), which are
32 presented in liquefaction potential relationship, are considered to have truncated exponential
33 probability density functions. It is important to note that the main deference between this paper
34 and the published papers is that the previous papers were followed the reliability assessment of
35 liquefaction by JDRV method using SPT, CPT and triaxial data (Johari, Javadi et al. 2012, Johari
36 and Khodaparast 2013, Johari and Khodaparast 2014). However, this research assesses this
37 reliability by JDRV method using shear wave velocity data.

38 2. Factor of Safety against liquefaction based on site shear wave velocity

39 The soil liquefaction Factor of Safety (FS) is defined in terms of Cyclic Resistance Ratio for
40 earthquakes with magnitude of 7.5 ($CRR_{7.5}$), Cyclic Stress Ratio (CSR), earthquake Magnitude
41 Scaling Factor (MSF), and overburden stress correction factor (K_σ) as:

$$42 \quad FS = \frac{CRR_{7.5}}{CSR} \cdot MSF \cdot K_\sigma \quad (1)$$

43 No liquefaction is predicted if $FS > 1$, and on the other hand, if $FS \leq 1$, liquefaction is predicted.
44 Cyclic Resistance Ratio for earthquakes with magnitude of 7.5 ($CRR_{7.5}$) can be obtained from shear
45 wave velocity measurement as (Andrus, Stokoe et al. 2004):

$$46 \quad CRR_{7.5} = K_{a2} \left\{ 0.022 \left(\frac{K_{a1} V_{S1cs}}{100} \right)^2 + 2.8 \left(\frac{1}{215 - (K_{a1} V_{S1cs})} - \frac{1}{215} \right) \right\} \quad (2)$$

1 where:

2 V_{S1cs} : The clean-sand equivalent of the overburden stress-corrected shear-wave velocity, defined
3 as (Andrus, Stokoe et al. 2004):

$$4 \quad V_{S1cs} = K_{cs} V_{S1} \quad (3)$$

5 V_{S1} : The stress-corrected shear-wave velocity normalized to the effective overburden stress of
6 100 kPa calculated as (Youd, Idriss et al. 2001):

$$7 \quad V_{S1} = V_s C_{VS} = V_s \left(\frac{P_a}{\sigma'_v} \right)^{0.25} \quad (4)$$

8 C_{VS} : A factor to correct the measured site velocity for σ'_v (a maximum C_{VS} value of 1.4 is applied
9 at shallow depths).

10 V_s : Site shear wave velocity(m/s)

11 K_{cs} : Fines content correction to adjust V_{S1} values to a clean soil equivalent. It can be approximated
12 using the following equation (Juang, Jiang et al. 2002):

$$13 \quad \begin{cases} K_{cs} = 1 & FC \leq 5\% \\ K_{cs} = 1 + (FC - 5)T & 5\% < FC < 35\% \\ K_{cs} = 1 + 30T & FC \geq 35\% \end{cases} \quad (5)$$

14 where:

$$15 \quad T = 0.009 - 0.0109 \left(\frac{V_{S1}}{100} \right) + 0.0038 \left(\frac{V_{S1}}{100} \right)^2 \quad (6)$$

16 FC : The average fines content.

17 K_{a1} and K_{a2} : Correction factors for cementation and aging (Andrus, Stokoe et al. 2004).

18 The factors K_{a1} and K_{a2} are included in Equation (2) to extend the original CRR-based shear wave
19 velocity equation by Andrus and Stokoe (2000) for uncemented Holocene-age soils to older soils.
20 The two correction factors are suggested because it is believed that two mechanisms influence
21 the position of the CRR-based shear wave velocity curve for older soils. The first mechanism
22 involves the effect of aging on V_{S1} . The second mechanism involves the effect of aging on CRR.
23 Both K_{a1} and K_{a2} are 1.0 for uncemented soils of Holocene age. For older soils, the values of K_{a1} and
24 K_{a2} were proposed by Andrus et al. (2004).

25 The Cyclic Stress Ratio (CSR) has been proposed by Seed and Idriss (1971) as:

$$26 \quad CSR = \left(\frac{\tau_{av}}{\sigma'_v} \right) = 0.65 \left(\frac{\sigma_v}{\sigma'_v} \right) \left(\frac{a_{max}}{g} \right) (r_d) \quad (7)$$

27 where:

28 σ'_v : Effective vertical stress

29 σ_v : Total vertical stress

30 τ_{av} : Average shear stress causing liquefaction

31 $(a_{max}/g)=\alpha$: Peak horizontal ground surface acceleration normalized with respect to acceleration
32 of gravity

33 r_d : Stress reduction factor

1 The stress reduction factor, r_d , provides an approximate correction for flexibility in the soil
 2 profile. There are several empirical relations for determination of r_d . The earliest and most widely
 3 used recommendation for assessment of r_d was proposed by Seed and Idriss (1971),
 4 approximated by Liao and Whitman (1986), and expressed in Youd and Idriss (2001) as:

$$5 \quad r_d = \frac{1.0 - 0.4113h^{0.5} + 0.04052h + 0.001753h^{1.5}}{1.0 - 0.4177h^{0.5} + 0.05729h - 0.006205h^{1.5} + 0.00121h^2} \quad (8)$$

6 where:

7 h : depth below ground surface (m)

8 The magnitude scaling factor, MSF, has been used to adjust the induced CSR during earthquake
 9 magnitude M_w to an equivalent CSR for an earthquake magnitude, $M_w=7.5$. The MSF is thus
 10 expressed as (Youd, Idriss et al. 2001):

$$11 \quad MSF = \left(\frac{M_w}{7.5} \right)^{-2.56} \quad (9)$$

12 M_w : earthquake magnitude

13 The overburden pressure correction factor, K_σ is used to adjust the cyclic resistance ratio where
 14 the overburden stresses are much greater than 100 kPa. This factor is defined by Idriss and
 15 Boulanger (2006):

$$16 \quad K_\sigma = 1 - C_\sigma \ln(\sigma'_v / P_a) \leq 1.0 \quad (10)$$

17 where:

$$18 \quad C_\sigma = \frac{1}{18.9 - 17.3D_R} \leq 0.3 \quad (11)$$

19 P_a : Atmospheric air pressure

20 D_R : Field relative density

21 For uncemented soils, Equation (1) can be rewritten based on equations (2) to (11) as follows:

$$22 \quad FS = \frac{CRR_{7.5}}{CSR} \cdot MSF \cdot K_\sigma = \frac{\left(0.022 \left(\frac{V_{S1cs}}{100} \right)^2 + 2.8 \left(\frac{1}{215 - V_{S1cs}} - \frac{1}{215} \right) \right) \left(1 - \frac{1}{18.9 - 17.3D_R} \ln \left(\frac{\sigma'_v}{P_a} \right) \right)}{0.65 \frac{\sigma_v}{\sigma'_v} \times \frac{a_{max}}{g} \times r_d \times (M_w / 7.5)^{2.56}} =$$

$$\frac{\left(0.022 \left(\frac{K_{cs} V_{S1}}{100} \right)^2 + 2.8 \left(\frac{1}{215 - K_{cs} V_{S1}} - \frac{1}{215} \right) \right) \left(1 - \frac{1}{18.9 - 17.3D_R} \ln \left(\frac{(\gamma_{sat} - \gamma_w)h}{P_a} \right) \right)}{0.65 \frac{\gamma_{sat}}{(\gamma_{sat} - \gamma_w)} \times \alpha \times r_d \times (M_w / 7.5)^{2.56}} \quad (12)$$

23 Equation (12) can be simplified as:

$$24 \quad FS(V_{S1}, r_d, \alpha, M_w) = \frac{L(V_{S1}) M_w^{-2.56}}{r_d \times \alpha} \quad (13)$$

25 where

$$L(V_{S1}) = \frac{\left(0.022\left(\frac{K_{cs} V_{S1}}{100}\right)^2 + 2.8\left(\frac{1}{215 - K_{cs} V_{S1}} - \frac{1}{215}\right)\right)}{0.65 \times \gamma_{sat} \times 7.5^{-2.56}} \frac{1}{(\gamma_{sat} - \gamma_w) \left(1 - \frac{1}{(18.9 - 17.3 D_R)} \ln\left(\frac{(\gamma_{sat} - \gamma_w) h}{P_a}\right)\right)} \quad (14)$$

It should be noted that if $\sigma'_v \leq 100$ kPa, then $K_\sigma = 1.0$ and the term $\left(1 - \frac{1}{18.9 - 17.3 D_R} \ln\left(\frac{(\gamma_{sat} - \gamma_w) h}{P_a}\right)\right)$ is removed from equation (14).

3. Developing relations between dependent variables

The jointly distributed random variables method that is used for reliability assessment in this research assumes that the variables are independent. There are several stochastic parameters in equations (13) and (14). As the liquefaction classification problem is highly nonlinear in nature, it is difficult to develop a comprehensive model taking into account all the independent variables, such as the seismic and soil properties, using conventional modeling techniques. Hence, in many of the conventional methods that have been proposed, simplified assumptions have been made.

No direct correlation exists between α and earthquake magnitude. Several empirical relationships have been developed for estimating α as a function of earthquake magnitude, distance from the seismic energy source, and local site conditions. Preliminary attenuation relationships have also been developed for a limited range of soft soil sites (Idriss 1991). Selection of an attenuation relationship should be based on such factors as the region of the country, type of faulting, and site condition (Youd, Idriss et al. 2001).

On the other hand, in equation (14), the parameters D_R and γ_{sat} are related to V_{S1} . In this section, the relationship between D_R and V_{S1} as well as γ_{sat} and V_{S1} are developed to resolve the dependency problem of variables in this equation. As a result of this derivation, equations (13) and (14) have four stochastic parameters, peak ground acceleration (α), earthquake magnitude (M_w), corrected shear-wave velocity (V_{S1}), and stress reduction factor (r_d) as well as the deterministic parameters maximum possible dry unit weight ($\gamma_{d,max}$), minimum possible dry unit weight ($\gamma_{d,min}$), unit weight of water (γ_w), average Fines Content (FC), and specific gravity (G_s).

3.1. Relation between D_R and V_{S1} :

Andrus et al. (2004) proposed the following relation between V_{S1cs} and $N_{1,60cs}$:

$$V_{S1cs} = 87.8 (N_{1,60cs})^{0.253} \quad (15)$$

where:

V_{S1cs} : The clean-sand equivalent of the overburden stress-corrected shear-wave velocity. It can be calculated from equation (3).

$N_{1,60cs}$: The clean-sand equivalent of the overburden stress-corrected SPT blow count defined as (Youd, Idriss et al. 2001):

$$N_{1,60cs} = a + b.N_{1,60} \quad (16)$$

where:

$N_{1,60}$: The corrected SPT blow count normalized to the effective overburden stress of 100kPa

1 a and b are coefficients to account for the effect of Fines Content (FC), defined as (Youd, Idriss et
 2 al. 2001):

$$3 \begin{cases} a = 0 & FC \leq 5\% \\ a = \exp[1.76 - (190/FC^2)] & 5\% < FC < 35\% \\ a = 5.0 & FC \geq 35\% \end{cases} \quad (17)$$

$$4 \begin{cases} b = 1 & FC \leq 5\% \\ b = [0.99 + (FC^{1.5}/1000)] & 5\% < FC < 35\% \\ b = 1.2 & FC \geq 35\% \end{cases} \quad (18)$$

5 Several relationships between relative density and SPT blow counts have been proposed in the
 6 literature (Tokimatsu and Seed 1987, Terzaghi 1996, Idriss and Boulanger 2008). Cubrinovski
 7 and Ishihara (1999) proposed a relationship between D_R and corrected SPT blow count as:

$$8 \quad D_R = \sqrt{\frac{N_{1,60}}{C_D}} \quad (19)$$

9 where:

$$10 \quad C_D = \frac{9}{(e_{\max} - e_{\min})^{1.7}} \quad (20)$$

11 e_{\max} : Maximum possible void ratio from laboratory experiment

12 e_{\min} : Minimum possible void ratio from laboratory experiment

13 The void ratio range ($e_{\max} - e_{\min}$) can be calculated as follows (Das 2013):

$$14 \quad e = \frac{G_s \gamma_w}{\gamma_d} - 1 \rightarrow \begin{cases} e_{\max} = \frac{G_s \gamma_w}{\gamma_{d_{\min}}} - 1 \\ e_{\min} = \frac{G_s \gamma_w}{\gamma_{d_{\max}}} - 1 \end{cases} \rightarrow e_{\max} - e_{\min} = \frac{G_s \gamma_w (\gamma_{d_{\max}} - \gamma_{d_{\min}})}{\gamma_{d_{\max}} \cdot \gamma_{d_{\min}}} \quad (21)$$

15 where:

16 $\gamma_{d_{\max}}$: Maximum possible dry unit weight from laboratory experiment

17 $\gamma_{d_{\min}}$: Minimum possible dry unit weight from laboratory experiment

18

19 Combining equations (15) to (19), the relationship between D_R and V_{s1} can be developed as:

$$20 \quad D_R = \left(\frac{1}{b \cdot C_D} \left(\frac{5K_{CS} V_{S1}}{439} \right)^{\frac{1000}{253}} - a \right)^{0.5} \quad (22)$$

21 3.2. Relation between γ_{sat} and V_{s1} :

22 The relation between γ_{sat} and γ_d can be derived from their basic definitions as (Das 2013):

$$\left. \begin{aligned} 1 \quad \gamma_{\text{sat}} &= \frac{(G_s + e)\gamma_w}{1 + e} \\ \gamma_d &= \frac{G_s \times \gamma_w}{1 + e} \rightarrow e = \frac{G_s \times \gamma_w}{\gamma_d} - 1 \end{aligned} \right\} \rightarrow \gamma_{\text{sat}} = \frac{\left(G_s \left(1 + \frac{\gamma_w}{\gamma_d} \right) - 1 \right) \gamma_d}{G_s} \quad (23)$$

2 where:

3 γ_{sat} : Saturated unit weight

4 γ_d : Dry unit weight in natural state of soil

5 G_s : Specific gravity of soil solids

6 γ_w : Unit weight of water (9.81 kN/m³)

7 e : Void ratio in natural state of soil

8 The relation between relative density (D_R) and dry unit weight (γ_d) is (Das 2013):

$$9 \quad D_R = \frac{\gamma_d - \gamma_{d_{\min}}}{\gamma_{d_{\max}} - \gamma_{d_{\min}}} \times \frac{\gamma_{d_{\max}}}{\gamma_d} \rightarrow \gamma_d = \frac{\gamma_{d_{\min}} \cdot \gamma_{d_{\max}}}{\gamma_{d_{\max}} - D_R (\gamma_{d_{\max}} - \gamma_{d_{\min}})} \quad (24)$$

10 Using equation (23) and (24), the relation between γ_{sat} and D_R can be developed as follows:

$$11 \quad \gamma_{\text{sat}} = \frac{\gamma_{d_{\max}} \cdot \gamma_{d_{\min}} (G_s - 1)}{G_s (\gamma_{d_{\max}} + (\gamma_{d_{\min}} - \gamma_{d_{\max}}) D_R)} \quad (25)$$

12 With substituting equation (22) in equation (25), the relation between γ_{sat} and V_{s1} can be
13 obtained as bellow:

$$14 \quad \gamma_{\text{sat}} = \frac{\gamma_{d_{\max}} \cdot \gamma_{d_{\min}} (G_s - 1)}{G_s \left(\gamma_{d_{\max}} + (\gamma_{d_{\min}} - \gamma_{d_{\max}}) \left(\frac{1}{b \cdot C_D} \left(\frac{5K_{cs} V_{s1}}{439} \right)^{\frac{1000}{253}} - a \right)^{0.5} \right)} \quad (26)$$

15 By substituting equation (22) and (26) into equations (13) and (14), these equations convert to a
16 stochastic independent variable relations.

17 4. Jointly distributed random variables method

18 Jointly distributed random variables method is an analytical stochastic method. In this
19 method, the probability density function (pdf) of input variables are expressed mathematically
20 and jointed together by statistical relations. The JDRV method is an exact method and can be used
21 for stochastic parameters with any distribution curve (such as normal, lognormal, exponential,
22 gamma, uniform, ...). This ability is very important because the peak horizontal earthquake
23 acceleration ratio (α) and earthquake magnitude (M_w), which are presented in Factor of Safety
24 against liquefaction relationship, are considered to have truncated exponential probability
25 density functions. The available statistical and probabilistic relations between random variables
26 are given in the literature (Hoel, Port et al. 1971, Tijms 2012, Ramachandran and Tsokos 2014).

27 In recent years this method has been applied to a number of geotechnical engineering
28 problems (Johari and Javadi 2012, Johari, Javadi et al. 2012, Johari, Fazeli et al. 2013, Johari and
29 Khodaparast 2013, Johari and Khodaparast 2014, Johari and khodaparast 2015).

1 **5. Monte Carlo simulation**

2 The simulation by Monte Carlo can solve problems by generating suitable random numbers
 3 (or pseudo-random numbers) and assessing the dependent variable for a large number of
 4 possibilities. The MCS involves the definition of the variables that generate uncertainty and
 5 probability density function (pdf); determination of the value of the function using variable values
 6 randomly obtained considering the pdf; and repeating this procedure until a sufficient number of
 7 outputs to build the pdf of the function. The number of required Monte Carlo trials is dependent
 8 on the desired level of confidence in the solution as well as the number of variables being
 9 considered (Harr 1987), and can be estimated from:

10
$$N = \left[\frac{d^2}{4(1-\varepsilon)^2} \right]^n \tag{27}$$

11 where:

12 N: Number of Monte Carlo trials

13 d: The standard normal deviate corresponding to the level of confidence

14 ε : The desired level of confidence (0 to 100%) expressed in decimal form

15 n: Number of variables

16 If the problem has n variables, the number of trials increases geometrically, according to power
 17 n.

18 **6. Reliability assessment by jointly distributed random variables method**

19 For reliability assessment of liquefaction potential and to account for the uncertainties, four
 20 independent input parameters have been defined as stochastic variables. The stochastic
 21 parameters are stress corrected shear-wave velocity (V_{s1}) and stress reduction factor (r_d), which
 22 are modeled using truncated normal probability density functions (pdf) and the peak horizontal
 23 earthquake acceleration ratio (α) and earthquake magnitude (M_w) which are considered to have
 24 truncated exponential probability density functions. The depth is regarded as a constant
 25 parameter.

26 For reliability assessment of liquefaction safety factor using the JDRV method, equation
 27 (13) is rewritten into terms of K_1 to K_7 as shown in equation (28). The terms K_1 to K_7 , are
 28 introduced in equation (29). The probability density function of each term is derived separately
 29 by equations (36) to (43). Derivations of these equations are presented in the Appendix 1.

30
$$FS(K_1, K_2, K_3, K_4) = K_1 \cdot K_2 \cdot K_3 \cdot K_4 = K_5 \cdot K_3 \cdot K_4 = K_6 \cdot K_4 = K_7 \tag{28}$$

31 where:

32
$$\left\{ \begin{array}{l} K_1 = L(V_{s1}) \\ K_2 = \frac{1}{r_d} \\ K_3 = M_w^{-2.56} \\ K_4 = \frac{1}{\alpha} \\ K_5 = K_1 \times K_2 \\ K_6 = K_5 \times K_3 \\ K_7 = FS = K_6 \times K_4 \end{array} \right. \tag{29}$$

Using the above mathematical functions for K_1 to K_7 and $f_{k_1}(k_1)$ to $f_{k_7}(k_7)$ a computer program was developed (coded in MATLAB) to determine the probability density function curve of liquefaction safety factor. In addition, for comparison, determination of the safety factor for liquefaction using the MCS was also coded in the same computer program.

MATLAB is a multi-paradigm numerical computing environment. MATLAB allows matrix manipulations, plotting of functions and data, implementation of algorithms, creation of user interfaces, and interfacing with programs written in other languages.

To show the ability of the proposed method an example is presented in the following sections.

7. Example

To demonstrate the efficiency and accuracy of the proposed method in determining the probability density function curve for the liquefaction safety factor and reliability assessment, an example problem with selected parameters values from literature (Gabriels, Snieder et al. 1987, Kramer 1996, Duncan 2000, Youd, Idriss et al. 2001, Marosi and Hiltunen 2004) is presented. The stochastic parameters with truncated normal and truncated exponential distributions are shown in Tables (1) and (2) respectively, and the deterministic parameters are given in Table (3).

Table (1) _ Stochastic parameters with truncated normal distribution

Parameters	Mean	Standard deviation	Minimum	Maximum
r_d	0.8565	0.0207	0.7737	0.9394
V_{s1}	180	8	148	212

Table (2) _ Stochastic parameters with truncated exponential distribution

Parameters	λ	Minimum	Maximum	Mean
M_w	2/3	5.5	8.0	6.418
α	10	0.2	0.4	0.269

Table (3) _ Deterministic parameters

Depth of water table(m)	Depth(m)	FC (%)	$\gamma_{d_{min}}$ (kN/m ³)	$\gamma_{d_{max}}$ (kN/m ³)	G_s
0.0	12.0	10.0	14.0	19.0	2.65

In order to compare the results of the presented method with those of the MCS, the final probability density and cumulative distribution curves for the factor of safety against liquefaction are determined using the same data and both methods. For this purpose, 10,000,000 generation points are used for the MCS. The results are shown in Figures (1) and (2).

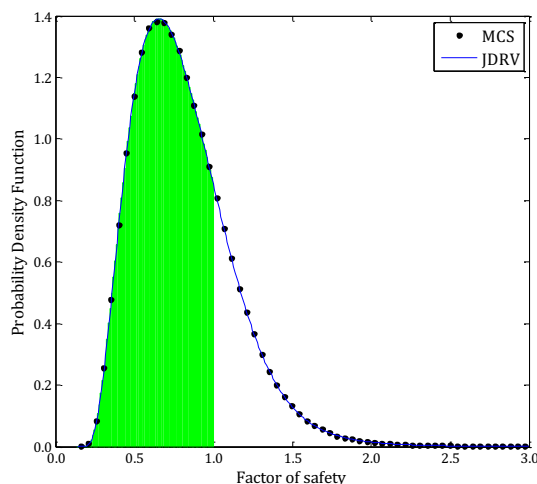


Figure (1) _ Comparison of probability density function of safety factor against liquefaction by two methods

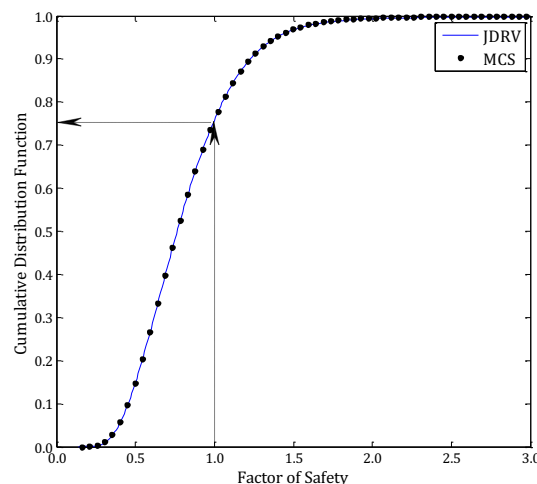


Figure (2) _ Comparison of cumulative distribution function of safety factor against liquefaction by two methods

As it can be seen in these figures, the results obtained using the developed method are very close to those of the MCS. The probability of liquefaction, is shown by green region for $FS < 1$, in Figure (1). Figure (2) shows the cumulative distribution curve of the liquefaction safety factor. It can be seen the probability of liquefaction ($FS \leq 1$) for this site at the assessed depth (12m) is about 76%. Table (4) indicates that at this depth liquefaction would most likely occur.

Table (4) _ Classes of liquefaction potential (Juang, Jiang et al. 2002)

Probability	Class	Description (Likelihood of liquefaction)
$0.85 < P_L < 1.00$	5	Almost certain that it will liquefy
$0.65 < P_L < 0.85$	4	Liquefaction very likely
$0.35 < P_L < 0.65$	3	Liquefaction and non-liquefaction equally likely
$0.15 < P_L < 0.35$	2	Liquefaction unlikely
$0.0 < P_L < 0.15$	1	Almost certain that it will not liquefy

On the other hand, a deterministic calculation using the mean value of the stochastic parameters shows that, the safety factor against liquefaction is about 0.72. This demonstrates that at this depth liquefaction would occur, but the probability of liquefaction is not specified. Therefore, the designer cannot have an engineering judgment. In fact, reliability assessment and engineering judgment are employed together to develop risk and decision analyses.

8. Probabilistic model development

8.1. Database

For developing the model, a database consisting of 225 site case histories, collected by Andrus et al. (1999), was used. The database is composed of 129 non-liquefied cases and 96 liquefied cases. Table (5) provides a summary of this database, including the ranges of parameter values of the case histories in the database.

Table (5) _ Parameters ranges of case histories in the database (Andrus, Stokoe et al. 1999)

Earthquake	M_w	a_{max} (g)	No. of cases		Depth (m)	G.W.L. (m)	FC (%)	V_{s1} (m/s)
			Liq.	Non-Liq.				
1906 SAN FRANCISCO, CALIFORNIA	7.7	0.32-0.36	8	4	4.6-9.9	2.4-6.1	5-44	124-191
1957 DALY CITY, CALIFORNIA	5.3	0.11	0	5	3.5-7.9	2.7-5.9	2-12	113-211
1964 NIIGATA, JAPAN	7.5	0.16	3	1	3.2-6.2	1.2-5.0	5	136-164
1975 HAICHENG, PRC	7.3	0.12	5	1	3.0-10.2	0.5-1.5	42-92	111-158
1979 IMPERIAL VALLEY	6.5	0.12-0.51	4	7	3.0-4.7	1.5-2.7	10-75	104-211
1980 MID-CHIBA, JAPAN	5.9	0.08	0	2	6.1-14.8	1.3	20-35	173-185
1981 WESTMORLAND, CALIFORNIA	5.9	0.02-0.36	6	5	3.0-4.7	1.5-2.7	10-75	104-211
1983 BORAH PEAK, IDAHO	6.9	0.23-0.46	15	3	1.9-3.7	0.8-3.0	5-6	115-318
1985 CHIBA-IBAARAGI, JAPAN	6.0	0.05	0	2	6.1-14.8	1.3	20-35	173-185
10/26/85 TAIWAN (EVENT LSST 2)	5.3	0.05	0	4	5.3-6.1	0.5	50	155-191
11/7/85 TAIWAN (EVENT LSST 3)	5.5	0.02	0	4	5.3-6.1	0.5	50	155-191
1/16/86 TAIWAN (EVENT LSST 4)	6.6	0.22	0	4	5.3-6.1	0.5	50	155-191
4/8/86 TAIWAN (EVENT LSST 6)	5.4	0.04	0	4	5.3-6.1	0.5	50	155-191
5/20/86 TAIWAN (EVENT LSST 7)	6.6	0.18	0	4	5.3-6.1	0.5	50	155-191
5/20/86 TAIWAN (EVENT LSST 8)	6.2	0.04	0	4	5.3-6.1	0.5	50	155-191
07/30/86 TAIWAN (EVENT LSST 12)	6.2	0.18	0	4	5.3-6.1	0.5	50	155-191
07/30/86 TAIWAN (EVENT LSST 13)	6.2	0.05	0	4	5.3-6.1	0.5	50	155-191
11/14/86 TAIWAN (EVENT LSST 16)	7.6	0.16	0	4	5.3-6.1	0.5	50	155-191
1987 CHIBA-TOHO-OKI, JAPAN	6.5	0.03	0	1	9.0	1.8	15	141
1987 ELMORO RANCH	5.9	0.03-0.24	0	11	3.0-4.7	1.8	10-75	104-211
1987 SUPERSTITION HILLS, CALIFORNIA	6.5	0.18-0.21	3	8	3.0-4.7	1.5-2.7	10-75	104-211
1989 LOMA PRIETA, CALIFORNIA	7.0	0.13-0.42	33	34	2.3-9.9	0.6-6.1	1-57	107-222
1993 KUSHIRO-OKI, JAPAN	8.3	0.41	2	0	4.2-4.5	0.9-1.9	5-7	161-189
1993 HOKKAIDO-NANSEI-OKI, JAPAN	8.3	0.15-0.19	3	1	2.0-7.0	1.0-1.4	5-54	99-166
1994 NORTHRIDGE, CALIFORNIA	6.7	0.51	3	0	4.4-5.6	3.4	10	142-170
1995 HYOGOKEN-NANBU, JAPAN	6.9	0.12-0.65	11	8	3.3-15	1.5-7.0	2-77	126-239
1906 SAN FRANCISCO, CALIFORNIA	7.7	0.32-0.36	8	4	4.6-9.9	2.4-6.1	5-44	124-191
1957 DALY CITY, CALIFORNIA	5.3	0.11	0	5	3.5-7.9	2.7-5.9	2-12	113-211
1964 NIIGATA, JAPAN	7.5	0.16	3	1	3.2-6.2	1.2-5.0	5	136-164

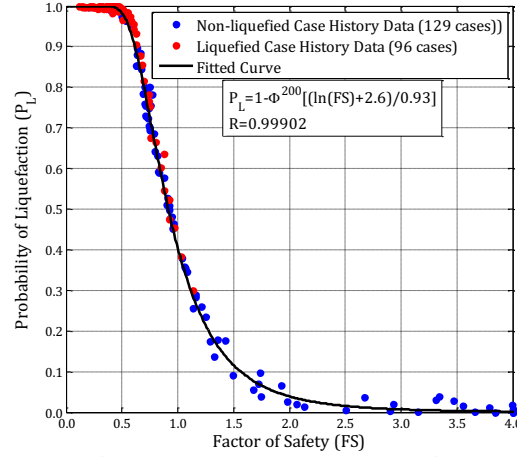
8.2. Model development

To develop the probabilistic liquefaction model the following procedure was followed:

- The uncertainty in the input parameters used in the calculation of safety factor of liquefaction was assessed for each series of database. The large majority of the

liquefaction case histories lack sufficient information to justify attempting to develop site-specific estimates of these uncertainties for each case history. For this reason, the COV of V_{s1} was taken as being the same for all case histories and equal to 0.05 as suggested by Marosi and Hiltunen (2004). The standard deviation of r_d was selected based on the three-sigma rule (Duncan 2000) and the curve suggested by Seed and Idriss (1971) for each depth. To consider the uncertainty of earthquake parameters, reasonable values were taken for the scale parameter of earthquake acceleration ratio and moment magnitude, as being the same for all case histories and equal to 0.05 and 0.8 respectively ($\beta_\alpha=0.05$ and $\beta_{M_w}=0.8$). Furthermore the range of variation of α and M_w was taken 0.2 and 2.5 respectively for all case histories ($M_{Wmax}-M_{Wmin}=2.5$ and $\alpha_{max}-\alpha_{min}=0.2$).

- The cumulative distribution function of each data series from the database was determined using the JDRV method as described in section 5.
- The probability of liquefaction was computed from the cumulative distribution function for each data series.
- The safety factor of each data series was calculated using the deterministic approach described in section 2.
- The probability of liquefaction and the related factor of safety from two previous steps were plotted with respect to each other for all data series. The results are shown in Figure (3).



Figure(3)_ Predictions of the developed probability liquefaction model using JDRV

- The probabilistic liquefaction model was developed using MATLAB curve fitting toolbox. The model has the following form:

$$P_L(FS) = 1 - \Phi^{200} \left[\frac{\ln(FS) + 2.6}{0.93} \right] \quad (30)$$

In equation (30), FS is computed using the method recommended by Andrus et al. (Andrus, Stokoe et al. 2004), as described in section 2 and Φ is the standard normal cumulative distribution function defined as:

$$\Phi(z) = \int_{-\infty}^z \frac{1}{\sqrt{2\pi}} \exp\left(-\frac{1}{2}u^2\right) du = \frac{1}{2} + \frac{1}{2} \operatorname{erf}\left(\frac{z}{\sqrt{2}}\right) \quad (31)$$

Using equation (31), equation (30) can be rewritten as:

$$P_L(FS) = 1 - \left[\frac{1}{2} + \frac{1}{2} \operatorname{erf}\left(\frac{\ln(FS) + 2.6}{0.93\sqrt{2}}\right) \right]^{200} \quad (32)$$

1 where erf is error function, defined as:

$$2 \operatorname{erf}(x) = \frac{2}{\sqrt{\pi}} \int_0^x \exp(-t^2) dt \quad (33)$$

3 8.3 Comparison of the model

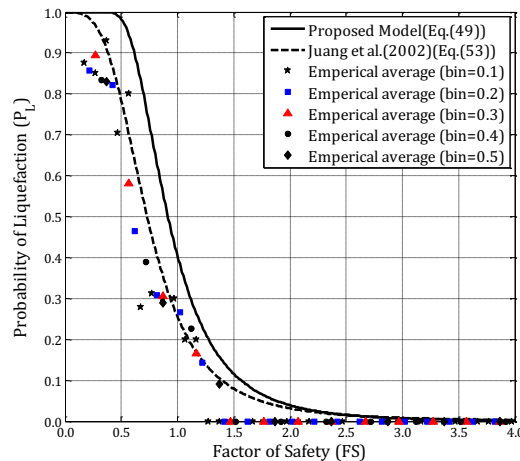
4 In this part the developed model was compared to an existing model and empirical data.
 5 For this purpose the model proposed by Juang et al. (2002) was selected.

$$6 P_L(FS) = \frac{1}{1 + \left(\frac{FS}{0.73}\right)^{3.4}} \quad (34)$$

7 where FS must be computed as suggested by Andrus and Stokoe (1997, 2000).

8 Additionally the model was compared with empirical data. For this purpose the FSs were
 9 calculated for all data using the deterministic approach as described in section 3. The results were
 10 then placed in different bin widths (classes) of 0.1, 0.2, 0.3, 0.4 and 0.5 based on their FS values.
 11 By counting the number of liquefied cases (n_1) and non-liquefied cases (n_2) in the same bin the
 12 empirical probability of liquefaction P_L corresponding to the center of each FS bin was obtained
 13 as $P_L = n_1 / (n_1 + n_2)$ (Juang, Ching et al. 2012).

14 Comparison of the probabilistic models proposed by JDRV and Juang et al. (2012) and the
 15 empirical data for bin widths 0.1, 0.2, 0.3, 0.4 and 0.5 is presented in Figure (4). Furthermore,
 16 liquefaction probability predictions of the models for some safety factors are given in Table (6).



Figure(4)_ Comparison of different models and empirical data

17

Table (6) _ Liquefaction probability predictions of the models

Model	Design FS	Probability of liquefaction (%)	
		Juang et al. (2002)	JDRV Model
Vs-based	1.0	25.54	40.46
	1.2	15.58	24.24
	1.5	7.95	11.58

18

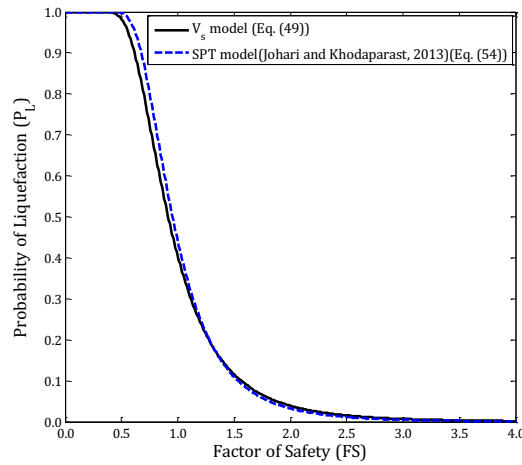
19 It can be seen that the proposed model provides a more conservative prediction of
 20 liquefaction potential than the Juang et al. (2002) model and empirical data which is due to use
 21 of liquefaction boundary curve proposed by Andrus and Stokoe (1997, 2000). This curve missed
 22 the least number of liquefied cases and thus is equivalent to the 26% probability curve (Juang,
 23 Jiang et al. 2002). This curve's conservation transfer to JDRV model directly. However, the Juang
 24 et al. (2002) model was derived using logistic regression and Bayesian mapping functions on
 25 shear wave velocity measurement database.

1 **8.4 Comparison of the V_s and SPT based probabilistic models**

2 A comparison of the results of the proposed model (Eq. (30)) and the SPT-based model
 3 developed using JDRV (Johari and Khodaparast 2013) (Eq. (35)) is presented in Figure (5).
 4

5
$$P_L(FS) = 1 - \Phi \left[\frac{\ln(FS) + 2.71}{0.89} \right] \quad (35)$$

6 In this equation, FS is computed using the method recommended by Youd and Idriss. (2001).
 7 It is shown that, as expected, the V_s -based model provides the more conservative prediction of
 8 liquefaction potential than the SPT-based model for important safety factors ($FS < 1.3$) (in the
 9 same probability of liquefaction occurrence, the V_s -based model predicts smaller factor of safety
 10 than SPT model) although the results of the models are close to each other.



Figure(5)_ Comparison of Vs and SPT based JDRV models

11 **9. Conclusion**

12 This paper has presented the development of a probabilistic model for liquefaction based
 13 on site shear wave velocity using the JDRV method. The Monte Carlo simulation was used for
 14 verifying the results of JDRV method. The selected stochastic parameters were stress-corrected
 15 shear-wave velocity and stress reduction factor, which were modeled using truncated normal
 16 probability density functions and the earthquake acceleration ratio and earthquake moment
 17 magnitude, which were considered to have truncated exponential probability density functions.
 18 The results showed that the probability distribution of the liquefaction safety factor obtained by
 19 the JDRV method is very close to that predicted by the Monte Carlo simulation. Moreover, the
 20 results indicated that the JDRV method was able to capture the expected probability distribution
 21 of the safety factor of liquefaction correctly. Comparison of the results of the proposed model
 22 and the SPT-based model, both developed using JDRV, shows that the V_s -based model provides a more
 23 conservative prediction of liquefaction potential than the SPT-base model.

24 **10. Appendix 1**

25 Derivation of mathematical functions K1 to K7 and FS and theirs domains is presented in this
 26 Appendix:

27
$$f_{K_1}(k_1) = f_{V_{s1}}(L^{-1}(k_1)) \times \left| \frac{d L^{-1}(k_1)}{d k_1} \right| = f_{V_{s1}}(V_{s1}) \times \left| \frac{1}{\frac{d K_1}{d V_{s1}}} \right| \quad (36)$$

1 $L(V_{S1_{\max}}) < k_1 < L(V_{S1_{\min}})$

2
$$\begin{cases} k_{1_{\min}} = L(V_{S1_{\max}}) \\ k_{1_{\max}} = L(V_{S1_{\min}}) \end{cases}$$

3

where:

4
$$\begin{cases} V_{S1_{\min}} = V_{S1_{\text{mean}}} - 4\sigma_{V_{S1}} > 0 \\ V_{S1_{\max}} = V_{S1_{\text{mean}}} + 4\sigma_{V_{S1}} \end{cases}$$

5 $V_{S1_{\text{mean}}}$: Average value of stress-corrected shear-wave velocity

6 $\sigma_{V_{S1}}$: Standard deviation of stress-corrected shear-wave velocity

7 $V_{S1_{\min}}$: Minimum value of stress-corrected shear-wave velocity

8 $V_{S1_{\max}}$: Maximum value of stress-corrected shear-wave velocity

9
$$f_{k_2}(k_2) = f_{r_d} \left(\frac{1}{k_2} \right) \left| \frac{d}{dk_2} \left(\frac{1}{k_2} \right) \right| = \frac{1}{\sigma_{r_d} \sqrt{2\pi} \cdot k_2^2} \exp \left(-0.5 \left(\frac{1 - r_{d_{\text{mean}}} \cdot k_2}{\sigma_{r_d} \cdot k_2} \right)^2 \right) \quad (37)$$

10 $r_{d_{\min}} \leq r_d \leq r_{d_{\max}} \rightarrow \frac{1}{r_{d_{\max}}} \leq k_2 \leq \frac{1}{r_{d_{\min}}}$

11
$$\begin{cases} k_{2_{\min}} = \frac{1}{r_{d_{\max}}} \\ k_{2_{\max}} = \frac{1}{r_{d_{\min}}} \end{cases}$$

12
$$\begin{cases} r_{d_{\min}} = r_{d_{\text{mean}}} - 4\sigma_{r_d} > 0 \\ r_{d_{\max}} = r_{d_{\text{mean}}} + 4\sigma_{r_d} \end{cases}$$

13 $r_{d_{\text{mean}}}$: Average value of stress reduction factor

14 σ_{r_d} : Standard deviation of stress reduction factor

15 $r_{d_{\min}}$: Minimum value of stress reduction factor

16 $r_{d_{\max}}$: Maximum value of stress reduction factor

17
$$f_{k_3}(k_3) = f_{M_w} \left(k_3^{\frac{-25}{64}} \right) \times \left| \frac{d}{dk_3} \left(k_3^{\frac{-25}{64}} \right) \right| = \frac{25 \times \lambda_{M_w} \cdot \exp(-\lambda_{M_w} k_3^{\frac{-25}{64}})}{64 \times k_3^{\frac{89}{64}} \left(\exp(-\lambda_{M_w} M_{w_{\min}}) - \exp(-\lambda_{M_w} M_{w_{\max}}) \right)} \quad (38)$$

18 $M_{w_{\min}} \leq M_w \leq M_{w_{\max}} \rightarrow (M_{w_{\max}})^{-2.56} \leq k_3 \leq (M_{w_{\min}})^{-2.56}$

19
$$\begin{cases} k_{3_{\min}} = (M_{w_{\max}})^{-2.56} \\ k_{3_{\max}} = (M_{w_{\min}})^{-2.56} \end{cases}$$

20

where:

21 $M_{w_{\min}}$: Minimum value of moment magnitude

22 $M_{w_{\max}}$: Maximum value of moment magnitude

23 λ_{M_w} : Rate of change in moment magnitude (rate parameter) $= 1/\beta_{M_w}$

24 β_{M_w} : Scale parameter of moment magnitude

$$1 \quad f_{K_4}(k_4) = f_\alpha\left(\frac{1}{k_4}\right) \left| \frac{d}{dk_4} \left(\frac{1}{k_4} \right) \right| = \frac{\lambda_\alpha \cdot \exp\left(-\frac{\lambda_\alpha}{k_4}\right)}{k_4^2 \cdot \exp(-\lambda_\alpha \cdot \alpha_{\min}) - \exp(-\lambda_\alpha \cdot \alpha_{\max})} \quad (39)$$

$$2 \quad \frac{1}{\alpha_{\max}} \leq k_4 \leq \frac{1}{\alpha_{\min}}$$

$$3 \quad \begin{cases} k_{4_{\min}} = \frac{1}{\alpha_{\max}} \\ k_{4_{\max}} = \frac{1}{\alpha_{\min}} \end{cases}$$

where:

5 α_{\min} : Minimum value of earthquake acceleration ratio

6 α_{\max} : Maximum value of earthquake acceleration ratio

7 λ_α : Rate of change in earthquake acceleration ratio (rate parameter) = $1/\beta_\alpha$

8 β_α : Scale parameter of earthquake acceleration ratio

$$9 \quad f_{K_5}(k_5) = f_{K_1 \times K_2}(k_5) = \int_{\alpha}^{\beta} |k_1| f_{K_1}(k_1) f_{K_2}\left(\frac{k_5}{k_1}\right) dk_1 \quad (40)$$

$$10 \quad k_{1_{\min}} k_{2_{\min}} \leq k_5 \leq k_{1_{\max}} k_{2_{\max}}$$

$$11 \quad \begin{cases} k_{5_{\min}} = k_{1_{\min}} k_{2_{\min}} \\ k_{5_{\max}} = k_{1_{\max}} k_{2_{\max}} \end{cases} \quad \text{and} \quad \begin{cases} \alpha = \max\left[k_{1_{\min}} \& \frac{k_5}{k_{2_{\max}}}\right] \\ \beta = \min\left[k_{1_{\max}} \& \frac{k_5}{k_{2_{\min}}}\right] \end{cases}$$

$$12 \quad f_{K_6}(k_6) = f_{K_5 \times K_3}(k_6) = \int_{\alpha}^{\beta} |k_3| f_{K_3}(k_3) f_{K_5}\left(\frac{k_6}{k_3}\right) dk_3 \quad (41)$$

$$13 \quad k_{5_{\min}} k_{3_{\min}} \leq k_6 \leq k_{5_{\max}} k_{3_{\max}}$$

$$14 \quad \begin{cases} k_{6_{\min}} = k_{5_{\min}} k_{3_{\min}} \\ k_{6_{\max}} = k_{5_{\max}} k_{3_{\max}} \end{cases} \quad \text{and} \quad \begin{cases} \alpha = \max\left[k_{3_{\min}} \& \frac{k_6}{k_{5_{\max}}}\right] \\ \beta = \min\left[k_{3_{\max}} \& \frac{k_6}{k_{5_{\min}}}\right] \end{cases}$$

$$15 \quad f_{K_7}(k_7) = f_{K_6 \times K_4}(k_7) = \int_{\alpha}^{\beta} |k_4| f_{K_4}(k_4) f_{K_6}\left(\frac{k_7}{k_4}\right) dk_4 \quad (42)$$

$$16 \quad k_{6_{\min}} k_{4_{\min}} \leq k_7 \leq k_{6_{\max}} k_{4_{\max}}$$

$$17 \quad \begin{cases} k_{7_{\min}} = k_{6_{\min}} k_{4_{\min}} \\ k_{7_{\max}} = k_{6_{\max}} k_{4_{\max}} \end{cases} \quad \text{and} \quad \begin{cases} \alpha = \max\left[k_{4_{\min}} \& \frac{k_7}{k_{6_{\max}}}\right] \\ \beta = \min\left[k_{4_{\max}} \& \frac{k_7}{k_{6_{\min}}}\right] \end{cases}$$

18 And the cumulative distribution function of K_7 can be determined as bellow:

$$19 \quad F_{K_7}(k_7) = P\{K_7 \in [k_{7_{\min}}, k_7]\} = \int_{k_{7_{\min}}}^{k_7} f_{K_7}(t) dt \quad (43)$$

1 $k_{7_{\min}} \leq k_7 \leq k_{7_{\max}}$

2 **11. References**

- 3 Alfredo, H.-S. A. and H. Wilson (1975). Probability concepts in engineering planning and design. John Wiley and Sons.
- 4 Andrus, R. D., P. Piratheepan, B. S. Ellis, J. Zhang and C. H. Juang (2004). Comparing liquefaction evaluation methods using
5 penetration-V S relationships. *Soil dynamics and earthquake engineering*. **24**: 713-721.
- 6 Andrus, R. D. and K. H. Stokoe II (2000). Liquefaction resistance of soils from shear-wave velocity. *Journal of Geotechnical
7 and Geoenvironmental Engineering*. **126**: 1015-1025.
- 8 Andrus, R. D. and K. H. Stokoe (1997). Liquefaction resistance based on shear wave velocity. Technical Report NCEER, US
9 National Center for Earthquake Engineering Research (NCEER). **97**: 89-128.
- 10 Andrus, R. D., K. H. Stokoe and R. M. Chung (1999). Draft guidelines for evaluating liquefaction resistance using shear
11 wave velocity measurements and simplified procedures, US Department of Commerce, Technology Administration,
12 National Institute of Standards and Technology.
- 13 Andrus, R. D., K. H. Stokoe and C. Hsein Juang (2004). Guide for shear-wave-based liquefaction potential evaluation.
14 *Earthquake Spectra*. **20**: 285-308.
- 15 Arulanandan, K., C. Yogachandran, N. J. Meegoda, L. Ying and S. Zhaui (1986). Comparison of the SPT, CPT, SV and
16 electrical methods of evaluating earthquake induced liquefaction susceptibility in Ying Kou City during the Haicheng
17 Earthquake. Use of in situ tests in geotechnical engineering, ASCE: 389-415.
- 18 Baziar, M. and N. Nilipour (2003). Evaluation of liquefaction potential using neural-networks and CPT results. *Soil
19 Dynamics and Earthquake Engineering*. **23**: 631-636.
- 20 Bolton Seed, H., K. Tokimatsu, L. Harder and R. M. Chung (1985). Influence of SPT procedures in soil liquefaction
21 resistance evaluations. *Journal of Geotechnical Engineering*. **111**: 1425-1445.
- 22 Chau, K.W. and C. L. Wu (2010). A Hybrid Model Coupled with Singular Spectrum Analysis for Daily Rainfall Prediction.
23 *Journal of Hydroinformatics*. **12** (4): 458-473.
- 24 Cubrinovski, M. and K. Ishihara (1999). Empirical correlation between SPT N-value and relative density for sandy soils.
25 **39**: 61-71.
- 26 Das, B. M. (2013). *Advanced soil mechanics*, CRC Press.
- 27 Dobry, R., K. Stokoe, R. Ladd and T. Youd (1981). Liquefaction susceptibility from S-wave velocity. ASCE National
28 Convention, ASCE New York, New York: 81-544.
- 29 Duncan, J. M. (2000). Factors of safety and reliability in geotechnical engineering. *Journal of geotechnical and
30 geoenvironmental engineering*. **126**: 307-316.
- 31 Gabriels, P., R. Snieder and G. Nolet (1987). In situ measurements of shear-wave velocity in sediments with higher-mode
32 Rayleigh waves. *Geophysical prospecting*. **35**: 187-196.
- 33 Goh, A. T. (2002). Probabilistic neural network for evaluating seismic liquefaction potential. *Canadian Geotechnical
34 Journal*. **39**: 219-232.
- 35 Harr, M.E. (1987). *Reliability-Based Design in Civil Engineering*. McGraw-Hill Book Company.
- 36 Hasofer, A., N. Lind and U. o. W. S. M. Division (1973). An exact and invariant first-order reliability format, University of
37 Waterloo, Solid Mechanics Division,.
- 38 Hoel, P. G., S. C. Port and C. J. Stone (1971). *Introduction to probability theory*, Houghton Mifflin Boston. **12**.
- 39 Idriss, I. (1991). Earthquake ground motions at soft soil sites. Second International Conference on Recent Advances in
40 Geotechnical Earthquake Engineering and Soil Dynamics (1991: March 11-15; St. Louis, Missouri), Missouri S&T
41 (formerly the University of Missouri--Rolla).
- 42 Idriss, I. and R. Boulanger (2006). Semi-empirical procedures for evaluating liquefaction potential during earthquakes.
43 *Soil Dynamics and Earthquake Engineering*. **26**: 115-130.
- 44 Idriss, I. and R. W. Boulanger (2008). *Soil liquefaction during earthquakes*, Earthquake engineering research institute.
- 45 Ishihara, K. (1996). *Soil behaviour in earthquake geotechnics*.

- 1 Johari, A., A. Fazeli and A. Javadi (2013). An investigation into application of jointly distributed random variables method
2 in reliability assessment of rock slope stability. *Computers and Geotechnics*. **47**: 42-47.
- 3 Johari, A. and A. Javadi (2012). Reliability assessment of infinite slope stability using the jointly distributed random
4 variables method. *Scientia Iranica*. **19**: 423-429.
- 5 Johari, A., A. Javadi, M. Makiabadi and A. Khodaparast (2012). Reliability assessment of liquefaction potential using the
6 jointly distributed random variables method. *Soil Dynamics and Earthquake Engineering*. **38**: 81-87.
- 7 Johari, A. and A. Khodaparast (2013). Modelling of probability liquefaction based on standard penetration tests using the
8 jointly distributed random variables method. *Engineering Geology*. **158**: 1-14.
- 9 Johari, A. and A. Khodaparast (2014). Analytical reliability assessment of liquefaction potential based on cone penetration test
10 results. *Scientia Iranica A*. **21**(5): 1549-1565.
- 11 Johari, A. and A. Khodaparast (2015). Analytical stochastic analysis of seismic stability of infinite slope. *Soil Dynamics and
12 Earthquake Engineering*. **79**: 17-21.
- 13 Juang, C. H. and C. J. Chen (1999). CPT-Based Liquefaction Evaluation Using Artificial Neural Networks. *Computer-Aided
14 Civil and Infrastructure Engineering*. **14**: 221-229.
- 15 Juang, C. H., C. J. Chen and T. Jiang (2001). Probabilistic framework for liquefaction potential by shear wave velocity.
16 *Journal of geotechnical and geoenvironmental engineering*. **127**: 670-678.
- 17 Juang, C. H., J. Ching, Z. Luo and C.-S. Ku (2012). New models for probability of liquefaction using standard penetration
18 tests based on an updated database of case histories. *Engineering Geology*. **133**: 85-93.
- 19 Juang, C. H., T. Jiang and R. D. Andrus (2002). Assessing probability-based methods for liquefaction potential evaluation.
20 *Journal of Geotechnical and Geoenvironmental Engineering*. **128**: 580-589.
- 21 Juang, C. H., S. H. Yang and H. Yuan (2005). Model uncertainty of shear wave velocity-based method for liquefaction
22 potential evaluation. *Journal of geotechnical and geoenvironmental engineering*. **131**: 1274-1282.
- 23 Juang, C. H., H. Yuan, D.-H. Lee and P.-S. Lin (2003). Simplified cone penetration test-based method for evaluating
24 liquefaction resistance of soils. *Journal of Geotechnical and Geoenvironmental Engineering*. **129**: 66-80.
- 25 Kramer, S. L. (1996). *Geotechnical earthquake engineering*, Prentice Hall Upper Saddle River, NJ. **80**.
- 26 Lees, J. J., R. H. Ballagh, R. P. Orense and S. V. Ballegooy (2015). CPT-based analysis of liquefaction and re-liquefaction
27 following the Canterbury earthquake sequence. *Soil Dynamics and Earthquake Engineering*, **79**(B): 304-314.
- 28 Liao, S. S. and R. V. Whitman (1986). Overburden correction factors for SPT in sand. *Journal of Geotechnical Engineering*.
29 **112**: 373-377.
- 30 Marosi, K. T. and D. R. Hiltunen (2004). Characterization of spectral analysis of surface waves shear wave velocity
31 measurement uncertainty. *Journal of geotechnical and geoenvironmental engineering*. **130**: 1034-1041.
- 32 Metropolis, N. and S. Ulam (1949). The monte carlo method. *Journal of the American statistical association*. **44**: 335-341.
- 33 Mitchell, J. K. and D.-J. Tseng (1990). Assessment of liquefaction potential by cone penetration resistance. *Proceedings of
34 the HB Seed Memorial Symposium*, Bi Tech Publishing. **2**: 335-350.
- 35 Morgenstern, N. (1995). Managing risk in geotechnical engineering. *Memorias del 10mo Congreso Panamericano de
36 Mecánica de Suelos e Ingeniería de Fundaciones*. **4**.
- 37 Muduli, P.K., S. K. Das and S. Bhattacharya (2014). CPT-based probabilistic evaluation of seismic soil liquefaction potential
38 using multi-gene genetic programming. *Georisk: Assessment and Management of Risk for Engineered Systems and
39 Geohazards*. Volume 8: 14-28.
- 40 Nafday, A. M. (2010). Soil liquefaction modelling by survival analysis regression. *Journal: Georisk: Assessment and
41 Management of Risk for Engineered Systems and Geohazards*. **4**: 77-92.
- 42 Ramachandran, K. M. and C. P. Tsokos (2014). *Mathematical Statistics with Applications in R*, Elsevier.
- 43 Robertson, P. (1990). Cone Penetration Testing for Evaluating Liquefaction Potential. *Proc., Symp. On Recent Advances
44 in Earthquake Des. Using Lab. And In Situ Tests*, ConeTec Investigations Ltd., Burnaby, BC, Canada.
- 45 Rosenblueth, E. (1975). Point estimates for probability moments. *Proceedings of the National Academy of Sciences*. **72**:
46 3812-3814.
- 47 Seed, H., K. Tokimatsu, L. Harder and R. Chung (1984). The Influence of SPT Procedures on Soil Liquefaction Resistance
48 Evaluations. Report no. UCB\ EERC-84/15. Earthquake Engineering Research Center, University of California, Berkeley,
49 CA.

- 1 Seed, H. B. and P. De Alba (1986). Use of SPT and CPT tests for evaluating the liquefaction resistance of sands. Use of in
2 situ tests in geotechnical engineering, ASCE: 281-302.
- 3 Seed, H. B., I. Idriss and I. Arango (1983). Evaluation of liquefaction potential using field performance data. Journal of
4 Geotechnical Engineering. **109**: 458-482.
- 5 Seed, H. B. and I. M. Idriss (1971). Simplified procedure for evaluating soil liquefaction potential. Journal of Soil Mechanics
6 & Foundations Div.
- 7 Seed, R. B. and L. F. Harder (1990). SPT-based analysis of cyclic pore pressure generation and undrained residual strength.
8 H. Bolton Seed Memorial Symposium Proceedings. **2**: 351-376.
- 9 Silver, M. L. (1977). Laboratory triaxial testing procedures to determine the cyclic strength of soils. Unknown. **1**.
- 10 Sowers, G. F. (1991). The human factor in failures. Civil Engineering—ASCE. **61**: 72-73.
- 11 Stokoe, K. H., J. Roesset, J. Bierschwale and M. Aouad (1988). Liquefaction potential of sands from shear wave velocity.
12 Proceedings, 9nd World Conference on Earthquake. **13**: 213-218.
- 13 Taormina, R., K. W. Chau and B. Sivakumar (2015). Neural network river forecasting through baseflow separation and
14 binary-coded swarm optimization. Journal of Hydrology. 529 (3): 1788-1797.
- 15 Terzaghi, K. (1996). Soil mechanics in engineering practice, John Wiley & Sons.
- 16 Tijms, H. (2012). Understanding probability, Cambridge University Press.
- 17 Tokimatsu, K. and H. B. Seed (1987). Evaluation of settlements in sands due to earthquake shaking. Journal of
18 Geotechnical Engineering. **113**: 861-878.
- 19 Tokimatsu, K. and A. Uchida (1990). Correlation between liquefaction resistance and shear wave velocity. **30**: 33-42.
- 20 Whitman, R. V. (2000). Organizing and evaluating uncertainty in geotechnical engineering. Journal of Geotechnical and
21 Geoenvironmental Engineering. **126**: 583-593.
- 22 Wu, C.L., K. W. Chau and C. Fan (2010). Prediction of rainfall time series using modular artificial neural networks coupled
23 with data-preprocessing technique. Journal of Hydrology. 389 (1-2): 146-167.
- 24 Youd, T., I. Idriss, R. D. Andrus, I. Arango, G. Castro, J. T. Christian, R. Dobry, W. L. Finn, L. F. Harder Jr and M. E. Hynes
25 (2001). Liquefaction resistance of soils: summary report from the 1996 NCEER and 1998 NCEER/NSF workshops on
26 evaluation of liquefaction resistance of soils. Journal of geotechnical and geoenvironmental engineering. **127**: 817-833.
- 27 Zou, H., S. Liu, G. Cai, T. V. Bheemasetti and A. J. Puppala (2017). Mapping probability of liquefaction using geostatistics
28 and first order reliability method based on CPTU measurements. Engineering Geology 218: 197-212.
- 29